REPORT DOCUMENTATION PAGE

Form Approved
OMB No. 0704-0188

1. REPORT DATE *(DD-MM-YYYY)*

2. REPORT TYPE
FINAL REPORT

3. DATES COVERED *(From - To)*
9/21/98 - 09/20/00

4. TITLE AND SUBTITLE
Meltwater Flowthrough Snow from Plot to Basin Scales

5a. CONTRACT NUMBER
DAAG55-98-1-0505

5b. GRANT NUMBER

5c. PROGRAM ELEMENT NUMBER

5d. PROJECT NUMBER

5e. TASK NUMBER

5f. WORK UNIT NUMBER

6. AUTHOR(S)
Williams, Mark; Pfeffer, W. Tad

7. PERFORMING ORGANIZATION NAME(S) AND ADDRESS(ES)
University of Colorado
INSTAAR
450 UCB
Boulder, CO 80309-0450

8. PERFORMING ORGANIZATION REPORT NUMBER
153-0330

9. SPONSORING/MONITORING AGENCY NAME(S) AND ADDRESS(ES)
U.S. Army Research Office
P.O. Box 12211
Research Triangle Park, NC 27709-2211

10. SPONSOR/MONITOR'S ACRONYM(S)

11. SPONSOR/MONITOR'S REPORT NUMBER(S)
ARO 39177.1-EV-RI

12. DISTRIBUTION/AVAILABILITY STATEMENT

13. SUPPLEMENTARY NOTES

14. ABSTRACT

This supplement provided funds to purchase two pieces of equipment for research in snow hydrology:

[1] High-precision temperature instrument suitable for snow.

[2] Denoth snow-wetness meters (2)

15. SUBJECT TERMS

16. SECURITY CLASSIFICATION OF:			17. LIMITATION OF ABSTRACT	18. NUMBER OF PAGES	19a. NAME OF RESPONSIBLE PERSON
a. REPORT	b. ABSTRACT	c. THIS PAGE			19b. TELEPHONE NUMBER *(Include area code)*

Standard Form 298 (Rev. 8/98)
Prescribed by ANSI Std. Z39.18

MEMORANDUM OF TRANSMITTAL

U.S. Army Research Office
ATTN: AMXRO-ICA-L (Hall)
P.O. Box 12211
Research Triangle Park, NC 27709-2211

___ Reprint (Orig + 2 copies)

___ Manuscript (1 copy)

___ Related Material (1 copy)

___ Technical Report (Orig + 2 copies)

_X_ Final Progress Report (Orig + 2 copies)

CONTRACT/GRANT NUMBER: DAAG55-98-1-0505

TITLE: Meltwater Flowthrough Snow form Plot to Basin Scales

is forwarded for your information.

SUBMITTED FOR PUBLICATION TO (applicable only if report is manuscript):

Sincerely,

Mark Williams

Final report:

EQUIPMENT SUPPLEMENT TO MELTWATER FLOW THROUGH SNOW FROM PLOT TO BASIN SCALES

M. W. Williams and W. T. Pfeffer

February 8, 2001

US Army Research Office: DAAG55-98-01-0505 supplement to DAAHO4-96-1-0033

Institution:
University of Colorado,
Boulder, Colorado.

FINAL REPORT

This supplement provided funds to purchase two pieces of equipment for research in snow hydrology:

[1] High-precision temperature instrument suitable for snow.

[2] Denoth snow-wetness meters (2)

High-precision temperature instrument

This supplement provided funds to purchase high-precision voltage measurement equipment for temperature measurements in snow column experiments. The experiments are directed toward distinguishing heat transfer via lattice conduction from heat transfer via vapor diffusion in snow columns, and were motivated in part by work published by S. Sokratov and others detailing observations of centimeter-scale heat sources and sinks revealed by quasi-steady-state temperature profiles.

These experiments are still being developed, with present work focussed on precise heater control for multiple snow columns. Our earlier apparatus was found to produce non-linear temperature profiles across the sample column (with the sample chamber filled with a non-reactive insulation) arising from lateral heat fluxes. The current prototype device consists of 8 6.5x6.5x18 inch snow sample chambers, with 16 thermostatically controlled heaters for temperature control, and temperature monitoring in the lateral directions as well as vertical. Once precise and stable linear temperature profiles are achieved in the columns without snow, we will proceed with snow measurements. The precision temperature measurement system will allow temperature profile measurements with accuracy approximately 2 orders of magnitude better than that achieved by Sokratov. we will also be able to perform temperature difference measurements across short grain chains using fine-wire differential thermocouples.

This ongoing work also involves Joel Harper (INSTAAR Post-Doctoral Research Associate), who is supported by an NSF Post-Doctoral Fellowship, and equipment is also supplemented by funds from that source.

Denoth snow-wetness meters (2)

Our field experimental program at Niwot Ridge is focussed on characterizing heterogeneity of water flow paths in snow. An essential part of this effort involves not only distinguishing wet snow from dry snow, but in evaluating liquid water content. We presently have a dielectric snow wetness measurement device manufactured in Finland by Martii Toikka, and a Denoth meter on loan from Dick Sommerfeld (USFS). The Denoth meter is the older and much more widely accepted of these two devices. The supplement allowed us to purchase two Denoth snow moisture meters.

Purchase of the Denoth meters has been a valuable aid in several snow experiments. Following is a draft manuscript involving the use of radar to visualize preferential flowpaths in snow. The draft manuscript provides an example of the type of measurements and experiments that we are doing with the Denoth snow wetness instrument.

Draft manuscript for *Hydrological Processes* January 5, 2001

IMAGING OF PREFERENTIAL FLOW PATHS IN A WET AND DRAINING SNOWPACK USING CROSSHOLE RADAR TOMOGRAPHY

Mark W. Williams
Department of Geography and
Institute of Arctic and Alpine Research,
University of Colorado, Boulder

Mike Knoll
Center for Geophysical Investigation of the Shallow Subsurface
Boise State University, Idaho

Corresponding Address†

Mark W. Williams
INSTAAR and Dept. of Geography
Campus Box 450
Boulder, CO 80309-0450
Telephone: 303/492-8830
Internet: markw@snobear.colorado.edu

ABSTRACT

Movement of liquid water through snowpacks is generally recognized to occur in distinct flow paths rather than as uniform flow through a homogeneous porous medium. Attempts to characterize the spatial distribution of preferential flowpaths have had only limited success. Most methods of investigating meltwater flow through snow involve sparse or invasive sampling. This makes it difficult to study scale and time-dependent processes such as the evolution of preferential flowpaths. Here we report on a proof-of-concept experiment conducted to evaluate the potential of crosshole radar tomography to image and characterize preferential flowpaths in snow. The experiment was conducted using a pulse radar system with 250 MHz borehole antennas, each placed in 3" PVC pipe, 5 m in length. One pipe was located at the bottom of the snowpack and the second at the top of the snowpack; both pipes were placed perpendicular to the fall line of the snow field. We purposely chose difficult conditions for the test, a wet and draining late-season snowpack. Travel velocities ranged by more than a factor of two, from about 125 m μs^{-1} to 300 m μs^{-1}, showing that material properties of the snowpack were influencing the propagation of radar waves through the snowpack. We then inverted the traveltime data to estimate the dielectric constant for each grid cell using a curved ray traveltime tomography algorithm. The estimated dielectric constants ranged from 1 to 4, similar to the 2.3 to 3.1 measured in a nearby snow pit using a Denoth Wetness Sensor. Conversion of the dielectric constants to liquid water content yield values of 1-3%, slightly less than the 1.5 to 4.5% estimated by the Denoth Wetness Sensor. The 20-20 cm spacing of vertical columns of higher liquid water content suggested by the crosshole radar tomography were on the same spatial scale as a concurrent dye tracer experiment.

INTRODUCTION

Movement of liquid water through snowpacks is one of the least understood aspects of snow hydrology [Richter-Menge and Colbeck, 1991]. It has an important influence on the timing and magnitude of snowmelt hydrographs [Caine, 1992] and on biogeochemical and geomorphological processes [Williams and Melack, 1989; Caine, 1995]. Adapting more physically-based approaches to understand and model flow through a snowpack should permit wider applications of operational snowpack models to more sites, and allow for year-to-year variability within a site [Melloh, 1999]. Similarly, research on glacial hydrology has shown that the least-understood part of this system is the simplistic way that current models treat meltwater storage and routing through supraglacial snowpacks [Arnold et al., 1998].

Movement of liquid water through snowpacks is generally recognized to occur in distinct flow paths rather than as uniform flow through a homogeneous porous medium. Seligman [1936] found that snowpack permeability was enhanced when flow channels were present in the snowpack. Oda and Kudo [1941] described flow fingers and flow along layer interfaces. Dye was used to trace flow paths during the Cooperative Snow Investigations [Gerdel, 1948; 1954; US Army, 1956]. Ice columns, described previously by Ahlmann and Tveten [1923], Ahlmann [1935], Seligman [1936], and Gerdel [1948], were recognized to be the residual flow network in cold snow by Sharp [1951]. Zones of preferential flow and ice columns have been observed in many other studies [e.g. Wankiewicz, 1976; Jordan, 1978; Denoth et al., 1979; Higuchi and Tanaka, 1982; Marsh, 1982 and 1988; Kattelmann, 1985 and 1986].

However, attempts to characterize the spatial distribution of preferential flowpaths have had only limited success [Marsh and Woo, 1985; Kattelmann, 1989; Kattelmann and Dozier, 1999]. Attempts to understand two-dimensional meltwater flow through snow from first principles have also had only limited success [Colbeck, 1979; 1991]. Overall, our ability to understand the spatial distribution of preferential flowpaths in melting snowpacks has suffered from the ephemeral nature of the flowpaths and the problems caused by destructive sampling of the snowpack [Schneebli, 1995; 1999; Albert et al., 1999].

Most methods of investigating meltwater flow through snow involve sparse or invasive sampling. This makes it difficult to study scale and time-dependent processes such as the evolution of preferential flowpaths. Imaging of internal snow pack properties using radar wavelengths shows promise as a non-invasive technique. The radar bandwidth has been used to detect surface and near-surface melting of snow [Koh, 1992; Koh and Jordan, 1995]. Radar reflection methods have been used to measure snowpack thickness and average water content [Annan et al., 1994]. Recently, Albert et al. [1999] demonstrated that flow paths in snow can be imaged by deploying radar antennas in snow trenches and orienting them so that they were most sensitive to reflections off vertical features. They were able to detect and map flow features as far as 1 m from trench faces using a Frequency Modulated Continuous Wave (FMCW) radar system in the 2-6 GHz range. Excavations confirmed that reflections were due to flow features in the snow pack. However the hydraulic properties of these flow features could not be determined without disturbing the snowpack.

Ground-penetrating radar (GPR) is a non-invasive geophysical technique that utilizes high-frequency (10 MHz-10 GHz) electromagnetic waves to image the subsurface [Davis and Annan, 1989]. In the past decade there has been a dramatic increase in the sophistication and number of GPR applications in hydrogeology, using both radar reflection profiling [Knoll et al., 1991; Peretti et al., 1999] and crosshole tomography [Hubbard et al., 1997]. Radar reflection profiling involves moving two, closely spaced, antennas together along a line and recording reflections from subsurface contrasts in dielectric properties. While this method is good for imaging sub-horizontal structures, it does not provide information on the material properties of a medium.

Crosshole radar tomography seems ideally suited to imaging and characterizing preferential flowpaths in snow. However, to the best of our knowledge it has never been applied to snow. Crosshole radar tomography involves inverting data from a multitude of transmission experiments with different source and receiver locations in two boreholes. The area between the boreholes is subdivided into cells to form the tomographic model domain. An inversion process is used to search for a set of model parameters that satisfy the system of equations representing the

tranmission experiments. In this way, crosshole tomography leads directly to material property estimates; the tomographic images also provide useful structural information. To illustrate, crosshole radar tomography has been used in hydrogeologic investigations to monitor the infiltration of fluids through the vadose zone, and to estimate soil hydraulic properties [Hubbard et al., 1997].

Here we report on a proof-of-concept experiment conducted to evaluate the potential of crosshole radar tomography to image and characterize preferential flowpaths in snow. The experiment was conducted at Niwot Ridge in the Colorado Front Range on 3 June 2000. We purposely chose difficult conditions for the test, a wet and draining late-season snowpack. Our objectives were: (1) to determine if the frequencies available for borehole antennas would be able to penetrate a wet and draining snowpack; (2) determine if their was sufficient change in the travel velocity of the radar waves to provide information on the material properties of snow; (3) to evaluate if "skipping" of radar waves at the snow/air interface would cause problems such that the technique could not be used; and (4) use this information to make an informed decision on the potential of crosshole radar tomography to image preferential pathways in seasonal snowpacks.

SITE DESCRIPTION

The experiment was conducted on the Niwot Ridge saddle at an elevation of 3,500 m, located in the Colorado Front Range of the Rocky Mountains about 5 km east of the Continental Divide (40° 03' N, 105° 35' W). This site is an UNESCO Biosphere Reserve and a Long-Term Ecological Research (LTER) network site. Climate is characterized by long, cool winters and a short growing season (1-3 months). Mean annual temperature is -3.8°C and annual precipitation is 1,000 mm [Williams et al., 1996]. About 80% of annual precipitation falls as snow [Caine, 1996].

The 2000 snow season at Niwot Ridge was characterized by below average snow deposition, a warm snow melt season with little precipitation, and early and continuous snow melt. By

the first week of June about 80% of the seasonal snow pack had melted. The experiment was conducted on a snow patch with dimensions of 50 m x 100 m. Slope angle of the experimental site was about 5°, with a SSE aspect.

METHODS

The experiment was conducted using a pulse radar system with 250 MHz borehole antennas, the highest frequency available (Figure 1). A snowpit was dug to the ground, approximately 2 m^2 in area. A PVC pipe, 3" id, was inserted horizontally at the bottom of the snowpack, in 1-m increments. As each pipe segment was inserted at the bottom of the snow pack, snow was removed from the pipe using a Federal snow sampler. We successfully inserted 5 m of pipe horizontally along the bottom of the snowpack, running perpendicular to the fall line. A second snow pit was then excavated to access the far end of the pipe. A second PVC pipe, also 3" id, was then laid on the surface of the snowpack, parallel to the pipe at the bottom of the snowpack. The snowpack was undisturbed between the two pipes. The end coordinates of the two pipes were measured relative to the NW corner of the top pipe. This allowed us to assign a position in space to each radar measurement.

The radar antennas were attached to ropes marked every 0.1 m and placed in the pipes. The snowpits were then backfilled to minimize potential problems caused by the snow-air interface. The borehole antenna in the top pipe was pulled over a distance of 5.0 m, with a measurement every 0.1 m. The bottom antenna was then moved 0.1 m and the top antenna again moved over the tracking distance of 5.0 m with a radar measurement every 0.1 m. The procedure was then repeated until the bottom antenna had moved 3.5 m. The length of the borehole antenna was 1.5 m. Consequently, when we refilled the snow pit, we could only pull the bottom antenna a distance of 3.5 m. We were thus able to measure radar waves using crosshole radar tomography every 0.1 m for a distance of 3.5 m for the bottom antenna and every 0.1 m for a distance of 5.0 m for the top antenna, a total of 1750 radar measurements with a variety of angles and crossing patterns.

Physical properties of the snowpack were measured in a snow pit approximately 10 m from the experimental site. Liquid water content of the snow was measured every 10 cm using a Denoth Wetness Sensor [Denoth et al., 1984; Williams et al., 1999a]. Snow density was sampled using a 1-L stainless steel cutter in vertical increments of 10 cm [Williams et al., 1999b]. Temperature of the snowpack was measured every 10 cm with 20-cm long dial stem thermometers, calibrated to ± 0.2°C using a one-point calibration at 0°C. Nearby dye was applied to the snow surface (Red Food Coloring #2) and the snowpack excavated an hour later in an independent attempt to visualize meltwater flow through snow during the experiment.

RESULTS

Field Experiment

Weather during the radar experiment on 3 June 2000 was warm and sunny. The experiment was conducted between 1 and 3 pm. Air temperature at 1 m height above the snow field was 10°C. Wind was less than 2 m s^{-1}. Cloud cover was less than 10%.

The radar experiment appeared to work in the field. Snow depth at the radar site was approximately 150 cm. We were able to pull the 250 MHz antennas through the pipes with little problem. The antenna in the pipe at the top of the snow pack was set in transmit mode and the antenna at the bottom of the snowpack was set in receiver mode. Real-time evaluation of the radar data in the field showed that we were receiving signals through the snow pack. More encouraging, there were differences in the wave speed of the first-arrival traveltimes for the crosshole radar data. These results showed that the 250 MHz radar waves were able to penetrate the snowpack, and that one or more material properties of the snowpack were causing differences in propagation of wave speeds through the snowpack.

Concurrent with the crosshole radar tomography experiment, we dug and analyzed a separate snow pit for snow properties (Figure 2). The analysis of the snow pit was conducted simultaneous with the radar imaging in a near-by location because the liquid water content can be

expected to change during the day under warm and sunny meteorological conditions. Snow depth of the pit was 150 cm. The snow pack was isothermal at 0°C. Snow grains were type 6b [Colbeck et al., 1990], melt-freeze polycrystals formed when water in veins froze. Density ranged from 470 to 550 kg m^{-3}, with a mean of about 500 kg m^{-3}. The dielectric constant as measured by the Denoth meter and corrected for snow density ranged from 2.3 to 3.1. The liquid water content ranged from 1.5 to 4.5% by volume. Snow density, dielectric constant, and liquid water content were all lower in the bottom 30 cm of the snowpack. This lowest 30 cm of the snowpack was old depth hoar (crystal type 4a) which had undergone wet metamorphism but still retained properties characteristic of depth hoar.

The red dye applied at the snow surface penetrated into the underlying snow with percolating meltwater. Visual analysis of the snowpack showed 5-7 horizontal layers in the top 20 cm of the snowpack, with vertical flow channels connecting the horizontal features (Figure 3). At snow pack depths greater than 50 cm below the snow surface, meltwater appeared to be concentrated in vertical flow channels spaced every 20-30 cm. Little dye was visible in the areas between the flow features, suggesting most of the surface melt was routed in preferential flowpaths. At a depth of about 1 m below the snow surface, dye was again spread laterally on a large ice lens. After breakthrough below this horizontal feature dye was again concentrated in preferential flow features.

Crosshole Radar Data Analysis

Travel velocities ranged by more than a factor of two, from about 125 m μs^{-1} to 300 m μs^{-1} (Figure 4). Note that in Figure 4, the area below the pipe is soil below the snowpack. These results show that there is also refraction of radar waves from soil below a wet and draining snowpack.

The wavespeeds suggest some problems with the radar technique. The striping at the top and sides of the wavespeed figure suggest problems at the snow-air interface. Similarly, the large area of high wave speed on the right side of the figure is where the snow pit had been refilled.

Air has a dielectric constant of 1 and a high velocity (300 m μs^{-1}). Consequently radar energy preferentially refracts through air rather than travel through the snow. The ray coverage needed for good tomographic inversion may be limited at the snow-air interface and also in snowpits that have been refilled. The quality of parameter estimates near the snow pits is thus suspect, but this doesn't affect results from the middle of the model, where we see the finger-like features extending down from the surface.

We then inverted the traveltime data to the dielectric constant for each grid cell using a curved ray traveltime tomography algorithm developed by Aldridge and Oldenburg [1993]. This algorithm reconstructs a two-dimensional velocity field from measured first arrival times by iteratively changing the model until the difference between observed and calculated traveltimes is reduced to an acceptable level. The inversion process includes a regularization matrix to stabilize the inversion process, perform a little spatial smoothing, and assign parameter values to cells that don't have any ray coverage (such as slow zones avoided by refracting rays). The forward modeling of traveltimes was then accomplished by Vidale's [1988] finite-difference scheme.

Here we only show the region between 0.75 m and 4.25 m, to get rid of most of the edge effects and model cells with low ray coverage (Figure 5). In an effort to improve parameter estimates, we including some spatial constraints in the tomographic inversion process. We forced values of the dielectric constant (ε) in the air to have a value of 1. We then used as a reference model with $\varepsilon = 1$ values near the snow pits to avoid local minima caused by extreme velocity contrasts near the edges of the models. These constraints help quite a bit, but the first constraint introduces a cyclical banding artifact in the upper 0.25 m that we haven't figured out how to eliminate yet.

Values for the calculated dielectric constant using crosshole radar tomography ranged from 1.0 to 4.0 (Figure 5). The range of these values is about twice that as measured by the Denoth Moisture Meter, which measured dielectric constants that ranged from 2.3 to 3.1. The crosshole radar tomography appears to produce reasonable values for the dielectric constant of undisturbed snow in a wet and draining snowpack.

We then converted the values for dielectric constant to liquid water content using the CRIM model, which is based on volumetric mixing of refractive indices (MIKE ref here):

$$\sqrt{\varepsilon_{measured}} = [Porosity\ x\ S_w\ x\ \sqrt{\varepsilon_{water}}] + [Porosity(1 - S_w)\ x\ \sqrt{(\varepsilon_{air})}] + [(1 - Porosity)\ x\ \sqrt{\varepsilon_{ice}}] \quad \text{Eq 1}$$

where $\varepsilon_{air} = 1$, $\varepsilon_{ice} = 3.2$, $\varepsilon_{water} = 87$ (0-5°C), and S_w is the water saturation. For this calculation, we assumed a constant density of 500 kg m^{-3}.

The calculated liquid water content (% per volume) ranged from 0 to 3% (Figure 6). The 0 to 3% liquid water content was similar to, though consistently less, than the 1-5% estimated using the Denoth Wetness Sensor.

The estimated spatial distribution of liquid water in the snow pack using crosshole radar tomography yields a pattern of relatively high liquid water content near the surface of the snow pack (light blue color). These high values of liquid water content appear to connect with relatively high liquid water content values at depths below 0.5 m. These vertical features are separated by areas of low (purple) water content about every 20-30 cm. These vertical columns of higher water content are consistent with the dye experiment in Figure 3. We interpret these vertical features in the undisturbed snow to be preferential flowpaths of percolating meltwater.

One surprising feature of the radar tomography is the apparent lack of horizontal stratigraphy. The horizontal features apparent in Figure 3 do not show up in the radar analysis. We do not know the reason for this apparent lack of stratigraphic information. A potential reason for the lack of stratigraphic information may be that the vertical scale of the ice lenses (< 1 cm in thickness) may be too small to be imaged, with radar measurements every 10 cm.

The higher liquid water content shown for the ground below the pipe in Figure 6 is also encouraging. The soil below the pipe contained a mixture of frozen and liquid water. These results suggest that crosshole radar tomography may provide information on the liquid water content of partially frozen soils.

DISCUSSION

Our proof-of-concept experiment suggests that crosshole radar tomography is a viable method for non-invasive imaging of the material properties of snow. The 250 MHz frequency available for borehole antennas was able to penetrate a wet and draining snowpack approximately 1.5|m in depth. The two-fold difference in traveltime velocities, ranging from about 125 m μs^{-1} to 300 m μs^{-1}, showed that material properties of the snowpack were influencing the propagation of radar waves through the snowpack and potentially providing usable information about these material properties.

We did experience some problems at snow-air interfaces, and also in snow pits that had been refilled. The radar waves appeared to "skip" at these interfaces. At these boundary areas the current inversion algorithms resulted in striping of the resultant images. Radar energy preferentially refracts through air rather than travel through the snow. The ray coverage needed for good tomographic inversion may be limited at the snow-air interface and also in snowpits that have been refilled.

Now that we know that crosshole radar tomography can image material properties of a snow pack, we can work on developing better models to invert traveltimes to material properties of snow. The algorithm by Aldridge and Oldenburg [1992] reconstructs a two-dimensional velocity field from measured first arrival times by iteratively changing the model until the difference between observed and calculated traveltimes is reduced to an acceptable level. The algorithm can also incorporate *a priori* model constraints into the inversion such as geostatistical information or known velocity values for specific cells. In the future we propose to use this capability to fix the velocity of model cells that we know something about the materials properties. Dielectric constant values for snow believed to be dry will be used to compute ice content and equivalent water content values using the Time Propagation mixing model [Knoll et al., in press]. Model cells we know to be air will be assigned a dielectric constant of 1. These model constrainsts should inprove the reliability of the model in areas that are extremely refractive.

Moreover, natural processes should create generate some common geostastical and petrophysical characteristics for things like flow fingers and ice columns. We should be able to map these probablistically (i.e., soft data), some better than others. For instance, dry high-porosity (low density) zones should be easy to map in tomography. Similarly, flow fingers in a dry snowpack should be easy to map using crosshole radar tomography.

Although the relationship between dielectric constant and volumetric moisture content is non-unique, the dielectric constant is much more sensitive to changes in liquid water content than it is to changes in porosity (MIKE, ref here). This is why empirical relationships like the Topp equation (MIKE, ref here) for soils work so well; the same should be true for snow. Also, hydrogeophysicists have shown that geophysical info can significantly improve hydraulic property estimates even when petrophysical relationships are non-unique and unknown (MIKE, ref here). Additional research efforts have a reasonable chance of being able to reconstruct estimates of the hydraulic properties of snow using non-invasive crosshole radar tomography.

ACKNOWLEDGEMENTS

Alex Machado and John Gartner provided invaluable field help. Funding was provided by grants from the Army Research Office (DAAH04-96-1-0033, DAAH04-96-0289, and DAAD19-00-1-0367), NSF Hydrology (EAR-9526875), the Niwot Ridge LTER program (NSF DEB 9810218), and NASA-EOS (NAGW-2602).

LITERATURE CITED

Ahlmann, H. W.. 1935. The stratification of the snow and firn on Isachsen's Plateau. Geografiska Annaler 17: 29-42.

Ahlmann, H. W. and A. Tveten. 1923. The recrystallization of snow into firn and the glaciation of the latter. Geografiska Annaler 5: 52-58.

Albert, M. R., G. Koh, and F. Perron. 1999. Radar investigations of melt pathways in a natural snowpack. Hydrologic Processes 13: 2991-3000.

Annan, A. P., S. F. Cosway, and T. Sigurdsson. 1994. GPR for snowpack water content. Proceedings of the 5th International Conference on Ground-Penetrating Radar, Waterloo, Ontario : 465-475.

Arnold, N., K. S. Richards, I. C. Willis, and M. J. Sharp. 1998. Initial results from a distributed, physically based model of glacier hydrology. Hydrological Processes 12: 191-219.

Caine, N.. 1992. Modulation of the diurnal streamflow response by the seasonal snowcover of an alpine basin. Journal of Hydrology 137: 245-260.

Caine, N.. 1995. Snowpack influences on geomorphic processes in Green Lakes Valley, Colorado Front Range. Geograph. Jour. 161: 55-68.

Caine, N.. 1996. Streamflow patterns in the alpine environment of North Boulder Creek, Colorado Front Range. Zeitschrift fur Geomorphologie 104: 27-42.

Colbeck, S. C.. 1979. Water flow through heterogeneous snow. Cold Regions Science and Technology 1: 37-45.

Colbeck, S. C.. 1991. The layered character of snow covers. Reviews of Geophysics 29: 81-96.

Colbeck, S. C., E. Akitaya, R. Armstrong, H. Gubler, J. Lafeuille, K. Lied, D. McClung, and E. Morris. 1990. The international classification for seasonal snow on the ground. National Snow and Ice Data Center.

Davis, J. L. and A. P. Annan. 1989. Ground-penetrating radar for high-resolution mapping of soil and rock stratigraph. Geophysical Prospecting 37: 531-551.

Denoth, A., A. Foglar, P. Weiland, C. Matzler, H. Aebischer, M. Tiuri, and A. Sihvola. 1984. A comparative study of instruments for measuring the liquid water content of snow. Journal of Applied Physics 56: 2154-2160.

Denoth, A., W. Seidenbusch, M. Blumthaler, P. Kirchlechner, W. Ambach, and S. C. Colbeck. 1979. Study of water drainage from columns of snow. CRREL Report 79-1. .

Gerdel, R. W.. 1948. Physical changes in snow cover leading to runoff, especially to floods. IAHS-AIHS Publication 31.

Gerdel, R. W.. 1954. The transmission of water through snow. Transactions, American Geophysical Union 35: 475-485.

Higuchi, K. and Y. Tanaka. 1982. Flow pattern of meltwater in mountain snow cover. p. 63-69. In J. W. Glen (ed.), Hydrological Aspects of Alpine and High-Mountain Areas. IAHS Publication No. 138 International Association of Hydrological Sciences.

Hubbard, S. S., J. E. Peterson, E. M. Majer, P. T. Zawislanski, K. H. Williams, J. Roberts, and F. Wobber. 1997. Estimation of permeable pathways and water content using tomographic radar data. The Leading Edge 16: 1623-1628.

Jordan, P.. 1978. The snowmelt hydrology of a small alpine watershed. M.S. Thesis. .

Kattelmann, R. C.. 1985. Macropores in snowpacks of Sierra Nevada. Annals of Glaciology 6: 272-273.

Kattelmann, R. C.. 1986. Measurements of snow layer water retention. In Cold Regions Hydrology Symposium. American Water Resources Association.

Kattelmann, R. C.. 1989. Spatial variability of snowpack outflow at a Sierra Nevada site. Annals of Glaciology 13: 124-128.

Knoll, M. D., F. P. Haeni, and R. Knight. 1991. Characterization of a sand and gravel aquifer using ground penetrating radar, Cape Cod, Massachusetts. USGS Water Resources

Investigation Report 91-4034. .

Knoll, M. D., R. Knight, and E. Brown. in press. Can accurate estimates of hydraulic permeability be obtained from measurements of dielectric properties. Geophysics .

Koh, G.. 1992. Effect of wind on FMCW radar backscatter from a wet snowcover. IEEE Transactions on Geoscience and Remote Sensing 30: 619-621.

Koh, G. and R. Jordan. 1995. Sub-surface melting in a seasonal snow cover. Journal of Glaciology 41: 474-482.

Marsh, P.. 1982. Ripening processes and meltwater movement in arctic snowpacks. Ph.D. Thesis. .

Marsh, P.. 1988. Flow fingers and ice columns in a cold snowcover. Proceedings of the Western Snow Conference 56: 105-112.

Marsh, P. and M.-k. Woo. 1985. Meltwater movement in natural heterogeneous snow covers. Water Resources Research 21: 1710-1716.

Melloh, R. A.. 1999. A synopsis and comparison of selected snowmelt algorithms. CRREL report 99-8. .

Oda, T. and K. Kudo. 1941. Properties of snow and its density. Seppyo 3: 109-121.

Peretti, W. R., M. D. Knoll, W. P. Clement, and W. Barrash. 1999. 3-D GPR imaging of complex fluvial stratigraphy at the Boise Hydrogeophysical Research Site. Symp. on the Appl. of Geophysics to Engineering and Environmental Problems (SAGEEP). .

Richter-Menge, J. A. and S. C. Colbeck. 1991. Recent progress in snow and ice research. Reviews of Geophysics, Supplement : 218-226.

Schneebeli, M.. 1995. Development and stability of preferential flow paths in a layered snowpack. p. 89-96. In K. A. Tonnessen, M. W. Williams, and M. Tranter (ed.), Biogeochemistry of Seasonally Snow Covered Basins. IAHS-AIHS Publication 228 International Association of Hydrological Sciences.

Seligman, G.. 1936. Snow Structure and Ski Fields. J. Adams.

Sharp, R.. 1951. Features of the firn on upper Seward Glacier, St. Elias mountains, Canada. Journal of Geology 59: 599-621.

US Army Corps of Engineers,. 1956. Snow Hydrology; Summary of Report of Snow Investigations. PB-151660. .

Vidale, J.. 1988. Finite-difference calculation of travel times:. BSSA 78: 2062-2076.

Wankiewicz, A.. 1976. Water percolation within a deep snowpack--Field investigations at a site on Mt. Seymour, British Columbia. unpublished Ph.D. dissertation. .

Williams, M. W., D. Cline, M. Hartman, and T. Bardsley. 1999b. Data for snowmelt model development, calibration, and verification at an alpine site, Colorado Front Range. Water Resources Research 35: 3205-3209.

Williams, M. W., M. Losleben, N. Caine, and D. Greenland. 1996a. Changes in climate and hydrochemical responses in a high-elevation catchment, Rocky Mountains. Limnology and Oceanography 41: 939-946.

Williams, M. W. and J. M. Melack. 1989. Effects of spatial and temporal variation in snow melt on nitrate and sulfate pulses in melt waters within an alpine basin. Annals of Glaciology 13: 285-289.

Williams, M. W., R. Sommerfeld, S. Massman, and M. Rikkers. 1999a. Correlation lengths of vertical flowpaths in melting snowpacks, Colorado Front Range, USA. Hydrologic Processes 13: 1807-1826.

FIGURE CAPTIONS

FIGURE 1. A 250 MHz antenna is being placed in the container pipe at the snow surface. In the foreground is the snowpit which provides access to the bottom antenna. The black wire is the lead from the bottom antenna.

FIGURE 2. Profiles of material properties of the snow pack measured by hand in a snow pit located about 10 m from the imaging site. Measurements of snow density, dielectric constant, and liquid water content were made concurrent with the radar measurements.

FIGURE 3. Vertical wall of a snow pit after red dye has percolated from the snow surface for about 1 hr. Note that the lower portion of the snow pack shows vertical dye features spaced 20-30 cm apart. We interpret these vertical dye features to be preferential meltwater flow channels.

FIGURE 4. Cross-sectional image of the radar wave velocities of a wet and draining snowpack. Black circles and stars show the transmitting and receiving antenna locations, respectively, within PVC pipes placed at the top and bottom of the snowpack. The area underneath the bottom pipe is partially frozen soil which is also returning a radar signal.

FIGURE 5. Cross-sectional image of the dielectric properties determined from tomographic inversion of crosshole radar traveltime data collected on Niwot Ridge on 3 June 2000. Note the dielectric constant values above 3 (greens mostly) at the top of the snowpack, and how these values connect up with localized zones of even higher dielectric constant values (yellows) at depths below 0.5 m; we interpret these funnel-shaped structures to be zones of high water content (i.e., preferential flow paths) within the late-stage snowpack.

FIGURE 6. Conversion of the dielectic properties in Figure 5 to volumetric liquid water content. The spacing of vertical flow features about every 20-30 cm is consistent with results from the dye experiment.

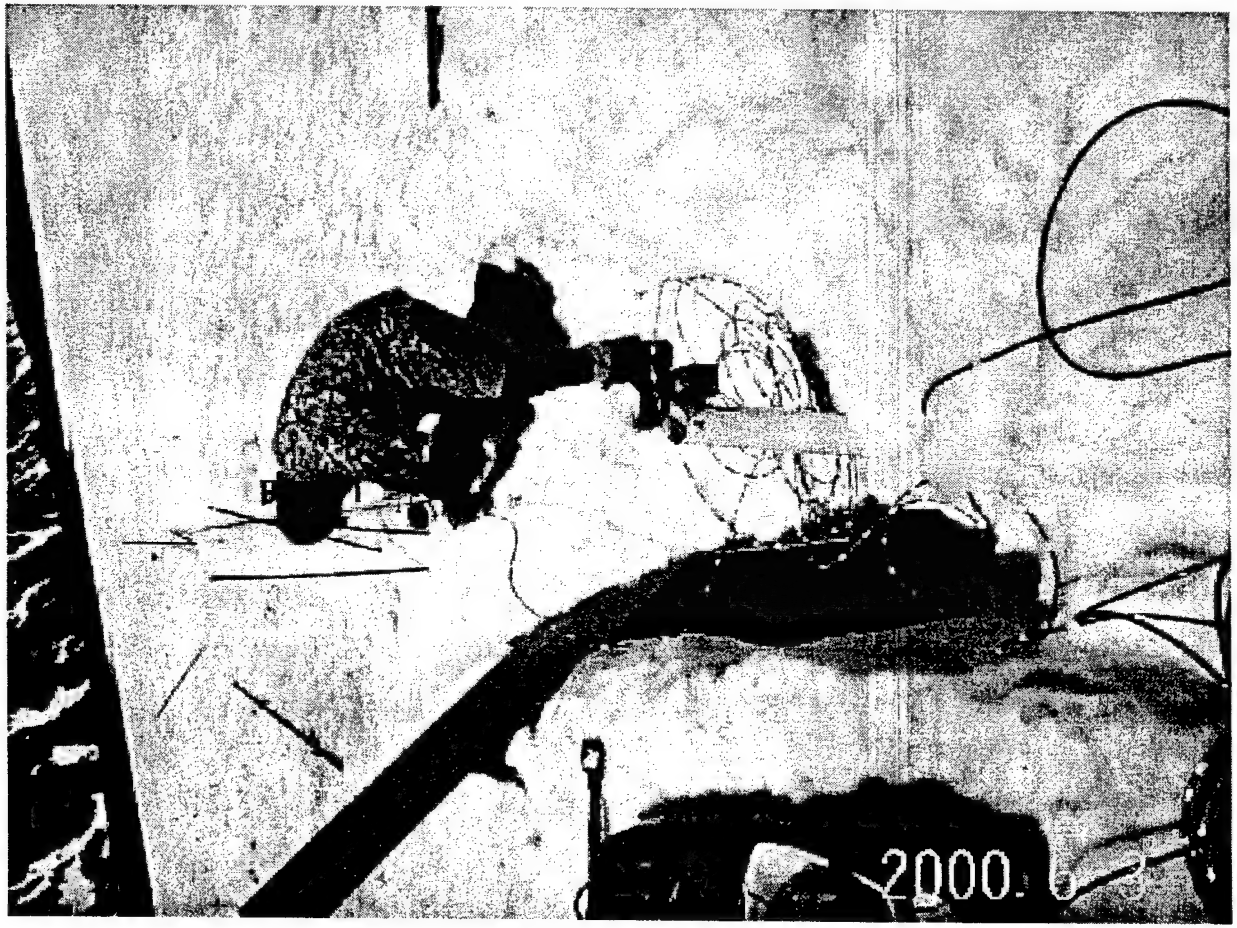
2000.

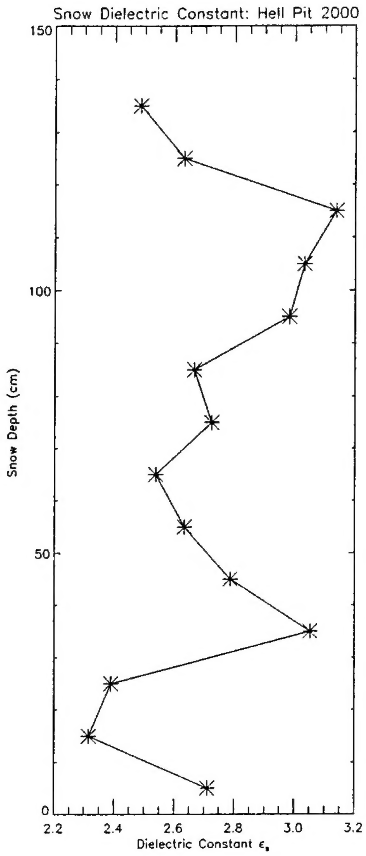

Snow Dielectric Constant: Hell Pit 2000
Snow Depth (cm)
Dielectric Constant ϵ_s

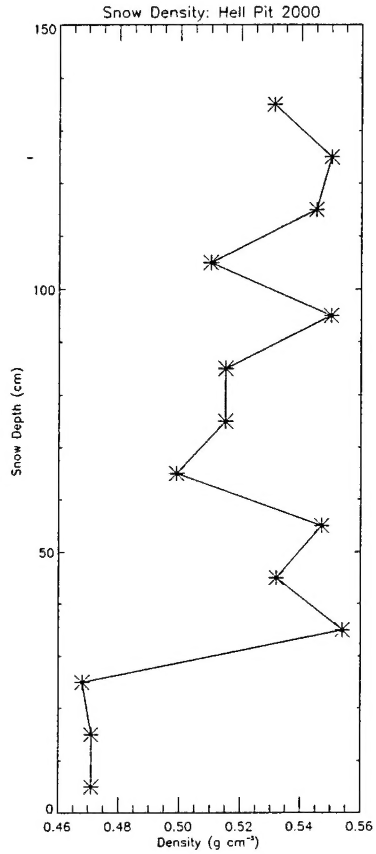

Snow Density: Hell Pit 2000
Snow Depth (cm)
Density (g cm^{-3})

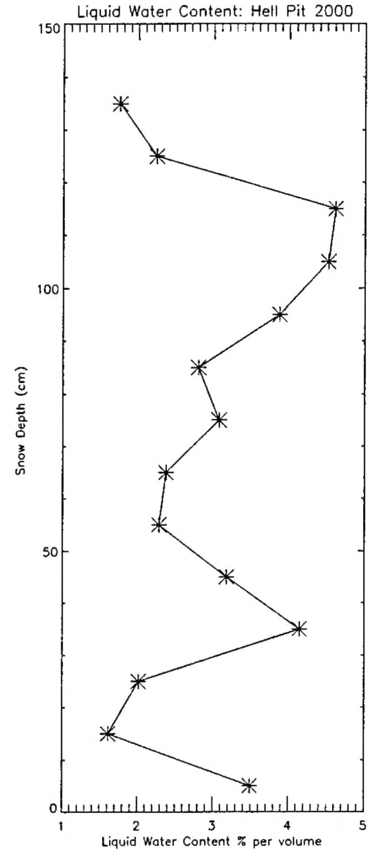

Liquid Water Content: Hell Pit 2000
Snow Depth (cm)
Liquid Water Content % per volume

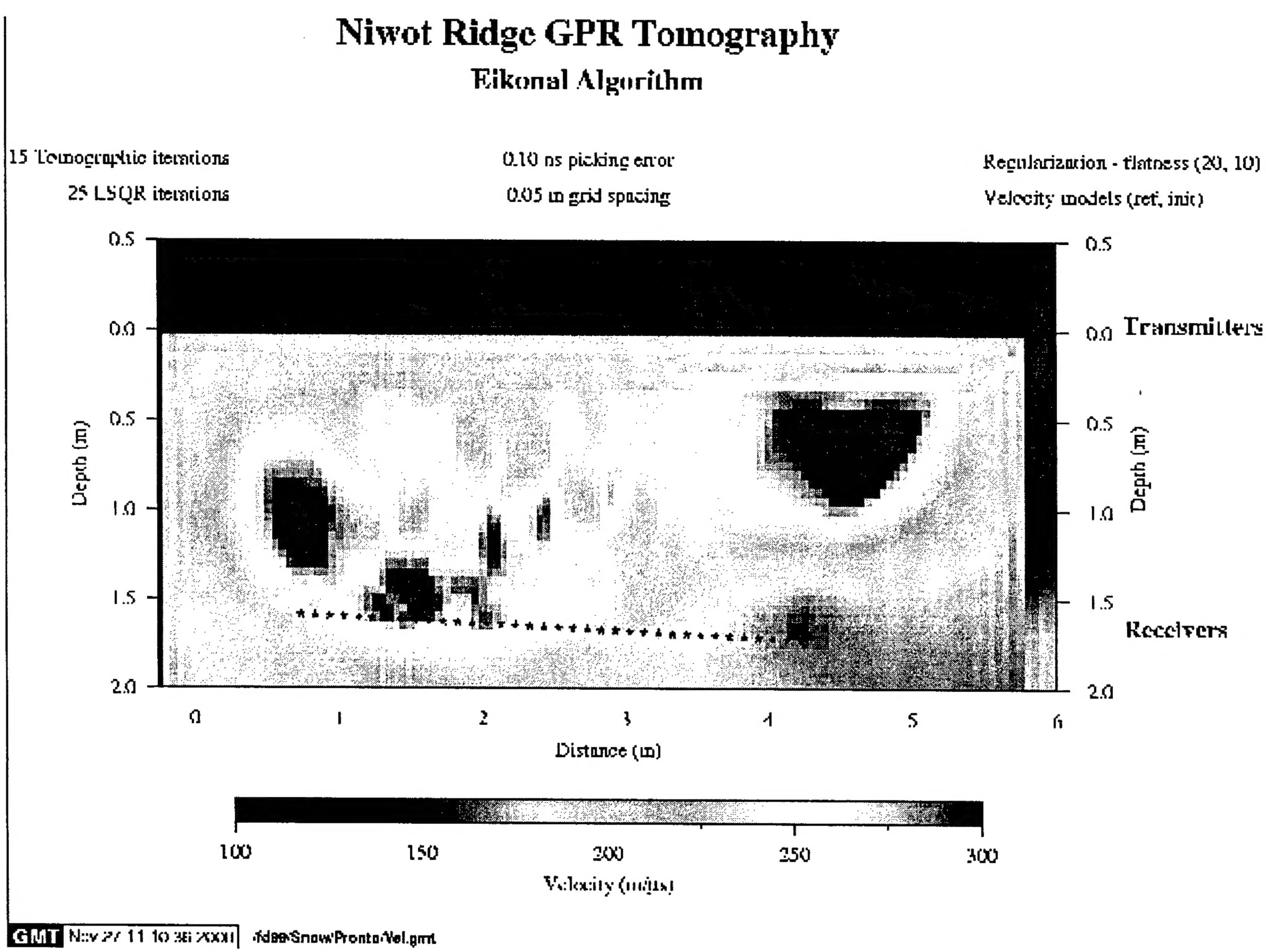

Niwot Ridge GPR Tomography
Eikonal Algorithm
15 Tomographic iterations
25 LSQR iterations
0.10 ns picking error
0.05 m grid spacing
Regularization - flatness (20, 10)
Velocity models (ref, init)
Depth (m)
Transmitters
Receivers
Distance (m)
Velocity (m/µs)
GMT

Niwot Ridge GPR Tomography

Eikonal Algorithm

15 Tomographic iterations | 0.10 ns picking error | Regularization - flatness (10, 10)

25 LSQR iterations | 0.05 m grid spacing | Velocity models (ref, init)

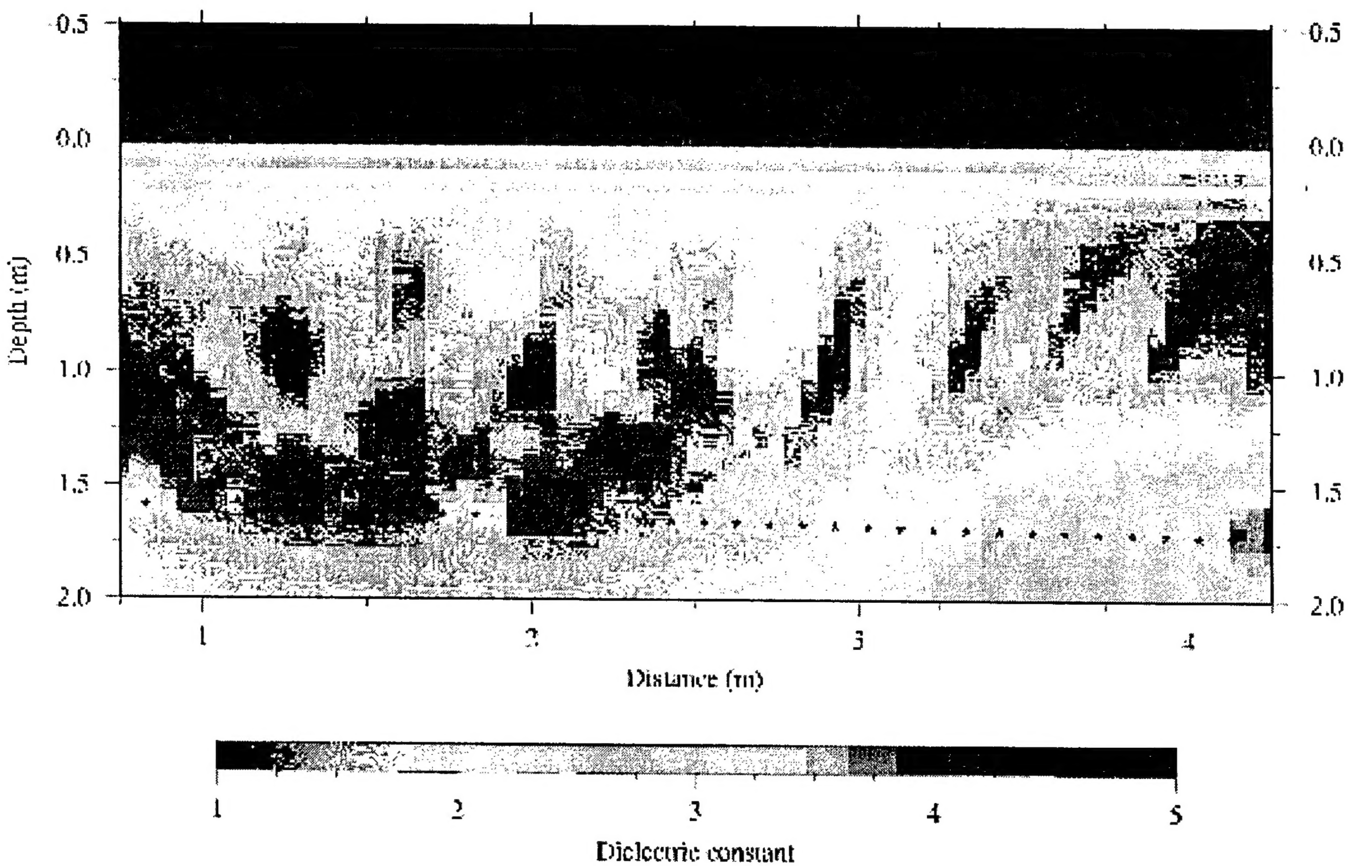

GMT Nov 27 12:10:13 2000 /d09/SnowPronto/Vel.gmt